Uncooled DWDM Using Orthogonal Coding for Low-Cost Datacommunication Applications

Johannes Benedikt von Lindeiner, *Student Member, OSA*, Jonathan D. Ingham, *Member, IEEE*, Adrian Wonfor, *Member, IEEE*, Jiannan Zhu, Richard V. Penty, *Senior Member, IEEE*, and Ian H. White, *Fellow, IEEE*

(Invited Paper)

***Abstract*—We describe a novel dense wavelength-division multiplexed systems (DWDM) system where by introducing orthogonality between adjacent channels and by using overlapping arrayed waveguide grating filter profiles, laser transmitters may operate without the need for thermoelecric cooling. Compared with a traditional DWDM system, a power consumption saving of up to 68% may be realized using this scheme. Results of a proof-of-principle 100 Gb/s (10 × 10 Gb/s) experiments that use alternating NRZ and Manchester (CAP-2Q) modulation is reported.**

***Index Terms*—Energy consumption, modulation coding, temperature control, wavelength division multiplexing.**

I. Introduction

With an increasing demand for high speed data connectivity emerging from an ever increasing consumer pool [1], standards such as the 40 and 100 Gb/s IEEE 802.3ba standards have been developed to alleviate pressure on existing networks [2]. Not only is it important to meet future demands, but it is also necessary to do so cost-effectively. Energy consumption and related operating costs are also important, not least as it is now expected that by 2020, carbon emission from data centers alone will exceed that of the airline industry [3]. It is also estimated that the networking industry already accounts for between 2–2.5% of global electricity consumption [4].

To meet future demand, operators are interested in using DWDM [5] in short haul datacommunication links. Currently however, much focus is on Coarse WDM as although DWDM brings higher performance, it is seen as an expensive technology owing to its need for expensive components that require tight spectral tolerances and control in order to avoid crosstalk between channels.

One of the key costs arising from the use of DWDM is the need for lasers at the transmitter to be temperature stabilized to maintain a constant wavelength through the use of Thermoelectric cooling (TEC) modules and wavelength lockers. This is required because otherwise, owing to the thermo-electric effect, wavelength channels will drift at a rate of ∼0.1 nm/°C [6]. Although one can often assume that for integrated sources, the wavelength channels drift collectively as the temperature gradient across the chip does not vary significantly, this may not always be the case and the situation may arise where wavelength channels drift to coincide. By overcoming the requirement of having a TEC along with supervisory/control system, a substantial power saving may be achieved. In addition, by no longer requiring tight wavelength stability, lasers that traditionally don't pass stability tests may be employed, these coming at a much reduced cost.

Various approaches have been devised to allow DWDM systems to operate without thermal control. These include the use of athermal tunable lasers [7] and the recently proposed uncooled multiple-input-multiple-output (MIMO) DWDM concept [8], [9]. Both techniques however require bespoke or advanced optical components and digital signal processing or control.

In this paper therefore, for the first time, we show how lasers at the transmitter may operate uncooled by using combinations of orthogonal coding schemes on alternating optical carriers combined with a receiving broad bandwidth cyclic arrayed waveguide grating (AWG). Individual receiving channels are designed to have overlapping profiles such that adjacent channels overlap with minimal insertion loss, allowing channels to be detected as they drift from one AWG passband to another under the influence of temperature. DWDM channels experience acceptable levels of penalty, even in the most challenging of situations. Such a system may therefore be well placed to overcome the challenges that traditional DWDM systems have faced in finding applications in low-cost datacommunications.

The remainder of the paper is organized as follows. In Section II we review the main systems aspects of uncooled orthogonal DWDM systems by looking at the use of broad bandwidth AWGs and novel orthogonal coding used to overcome crosstalk issues. Additionally, we compare the power consumption of the proposed system with other DWDM solutions. Section III describes a previously reported [10] proof-of principle experiment

Manuscript received June 20, 2014; revised September 16, 2014, December 1, 2014, and January 17, 2015; accepted January 17, 2015. Date of publication January 27, 2015; date of current version February 17, 2015. This work was supported by the Engineering and Physical Science Research Council (EPSRC) via the INTERNET project.

J. B. von Lindeiner is with the Centre for Photonic Systems, Department of Engineering, University of Cambridge, Cambridge CB3 0FA, U.K. and also with the Alcatel-Lucent Bell Labs, Murray Hill, NJ 08904 USA (e-mail: johannes.von_lindeiner@alcatel-lucent.com).

J. D. Ingham is with the Centre for Photonic Systems, Department of Engineering, University of Cambridge, Cambridge CB3 0FA, U.K. He is also with the Avago Technologies, San Jose, CA 95131, USA (e-mail: jdi21@cam.ac.uk).

A. Wonfor, J. Zhu, R. V. Penty, and I. H. White are with the Centre for Photonic Systems, Department of Engineering, University of Cambridge, Cambridge CB3 0FA, U.K. (e-mail: aw300@cam.ac.uk; jz333@cam.ac.uk; rvp11@cam.ac.uk; ihw3@cam.ac.uk).

Color versions of one or more of the figures in this paper are available online at http://ieeexplore.ieee.org.

Digital Object Identifier 10.1109/JLT.2015.2395351

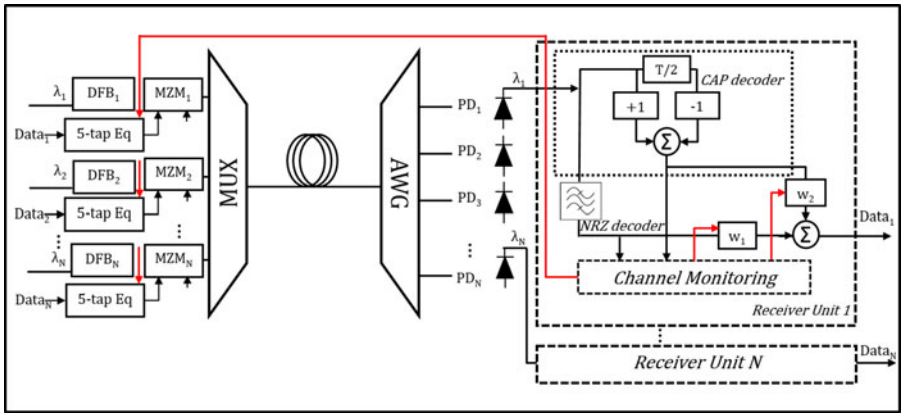

Fig. 1. 16-channel Orthogonal DWDM System Schematic.

of a 100 Gb/s aggregate DWDM experiment using 10 × 10 Gb/s channels with alternating non-return-to-zero (NRZ) and Manchester (CAP-2Q) coding where Q stands for the quadrature component of a CAP signal. Furthermore, we describe experimental results proving the feasibility of using discrete lasers by introducing a bias control mechanism aided by a simple pilot tone scheme. This allows situations where channels drift at different rates to be accommodated. Finally, we offer a conclusion in Section IV.

II. Orthogonal DWDM System Aspects

The system concept is illustrated in Fig. 1 which shows an N-channel orthogonal DWDM system. Such a system may operate as follows:

N directly (DML) or externally (EML) modulated lasers on a DWDM wavelength grid are encoded using alternating in-phase and quadrature-phase channels that form orthogonal pairs. These may comprise NRZ and CAP-2Q signals or multi-level amplitude modulation signals such as pulsed amplitude modulation (PAM-m) and CAP-mQ, where m represents the number of levels used to encode a bit stream. CAP-Q signal generation is realized using a 5-tap transversal filter in order to allow low-power operation and phase shifters are included to allow for temporal alignment between alternating channels. Signals are then transmitted over standard single mode fiber (SMF) after which they are detected by photodiode receivers at the output of a broad bandwidth cyclic AWG for which an example 4 channel spectrum is shown in Fig. 2. For each channel, the receiver comprises both a CAP-Q demodulator, which consists of a differential amplifier (2-tap $+1$ and -1 transversal filter) and an NRZ demodulator (low-pass filter). As will be shown in subsequent sections, by introducing pilot tones at between 10–200 kHz on carriers with a modulation index of 10%, channel identification at the receiver can take place allowing signals to be correctly routed using simple electronics without the need for high-power DSP.

A. Broad Bandwidth Cyclic AWG

In a typical DWDM system, the receiving AWG filter channels are fixed to the ITU grid and have narrow passbands with sharp roll-offs to avoid crosstalk from neighboring channels. Here, as shown in Fig. 2, the filter profile of these receiving channels may be increased to 100 GHz or beyond with a slow roll-off such that neighboring filter channel profiles have crossing points at approximately -3 dB for 100 GHz and -0.5 dB for 150 GHz. This allows channels to be detected with minimal insertion loss even once they have drifted outside the passband of the filter that had previously encompassed it. The cyclical properties of an AWG are exploited so that channels that drift outside the free spectral range of the AWG will instead of being lost, simply wrap around to the first detection channel. This allows multiple frequency bands to be detected without needing additional receivers. This is illustrated in Fig. 2 below, where if a channel drifts past $+300$ GHz, it wraps around and is detected by the cyclical channel centered at -200 GHz, shown as dotted lines.

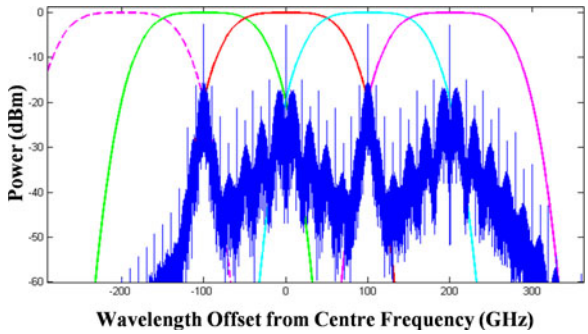

Fig. 2. Proposed AWG Profile with alternating NRZ and CAP-2Q channels.

Previous iterations [8] of this AWG profile have been employed to forgo the use of TECs at the transmitter. However, there, signals suffer from high levels of crosstalk owing to the slow roll-off of the AWGs resulting in the need for DSP-based crosstalk cancellation units to be deployed. Furthermore, receiver diversity, i.e., where the number of receiving filters exceeds the number of transmit channels, is necessary to avoid points of singularity as channels drift towards AWG crossing points. The approach in this paper improves functionality as both DSP and diversity isn't required. Channel decoding is readily possible even with the prevalence of high crosstalk levels.

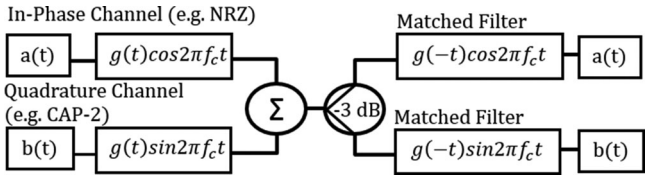

Fig. 3. CAP Transceiver Model.

B. Orthogonal Coding

In order to overcome transmission distance and spectral efficiency limitations inherent to NRZ modulation, researchers have sought alternative schemes [11] to address these issues. More complex encoding schemes such as multi-level pulse amplitude modulation (PAM-m) [11], quadrature amplitude modulation (QAM), orthogonal frequency division multiplexing (OFDM) and more recently CAP [12], [13] have been studied, with the last three modulation schemes classed as being different forms of orthogonal coding. OFDM, which though it may be detected using IM/DD receivers, requires computationally intensive operations, namely the Fourier and inverse Fourier transform. This typically requires significant power consumption, making the scheme undesirable for low-cost applications.

CAP on the other hand, an analogous form of QAM which arises from use in asymmetric digital subscriber line (ADSL) systems [14] is garnering greater attention as of late, owing to its ease of implementation and enhanced spectral efficiency. Whereas in QAM, where two separate signals are encoded using phase and amplitude modulation, CAP signals achieve their orthogonality temporally using different pulse shapes. Signals are generated and decoded using simple, low-cost, low-power transversal filters, generally requiring $<$10 mW in standard CMOS [15].

A typical model for generating and decoding a CAP signal is given in Fig. 3:

Two separately encoded signals, a (t) and b (t) are fed to two separate 5-tap transversal filters, where tap coefficients are set such that their responses form orthogonal pairs. $g(t)$, a square-root-raised-cosine response is multiplied by two orthogonal functions, $\cos 2\pi \mathrm{f_c t}$ and $\sin 2\pi \mathrm{f_c t}$. The minimum carrier frequency $\mathrm{f_c}$ is given by $\frac{F_s(1+\alpha)}{2}$, where F_s is the signal sampling rate and α is the roll-off. The outputs of the two transversal filters are then combined, wherein now the in-phase and quadrature channels occupy the same nominal carrier frequency, ideally without any interference. The transversal filter impulse responses are shown in Fig. 4 below.

After detection, matched filters may be used to extract the originally transmitted in-phase and quadrature data.

Simulated eye diagrams of a 10 Gb/s in-phase (NRZ), quadrature (CAP-2Q) signal and a composite eye signal are shown in Fig. 5. Additionally, a 25 Gb/s in-phase (PAM-4), quadrature (CAP-4Q) and composite CAP-16 signal is shown in Fig. 6.

Previous implementations of the aforementioned MIMO WDM systems [8] with overlapping AWG channels uses the same modulation scheme on each channel and therefore result in significant levels of crosstalk as channels begin to drift away from their optimum operating points. As they drift away, crosstalk increases and must be cancelled. This is accomplished using a DSP-based MMSE crosstalk cancellation unit, which eliminates contributions of one signal from the other. It should be noted that if all channels drift in one direction so that all sit on different AWG crossing points, crosstalk cancellation is not necessarily possible and hence additional receiver channels are added.

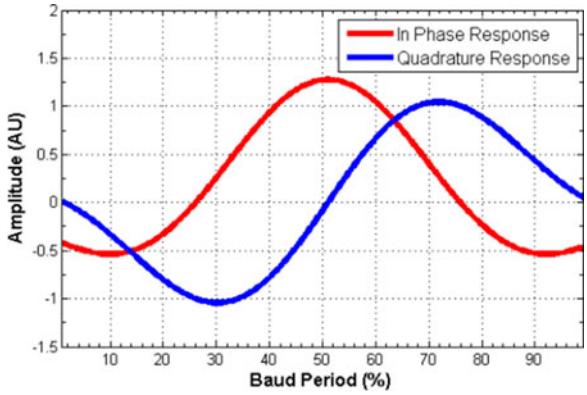

Fig. 4. Impulse responses of NRZ and CAP-2Q channels.

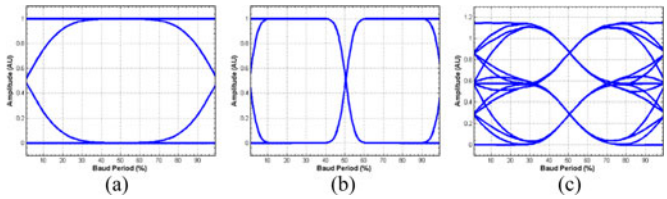

Fig. 5. Eye diag. of 10 Gb/s (a) NRZ (b) CAP-2Q (c) 20 Gb/s composite signal.

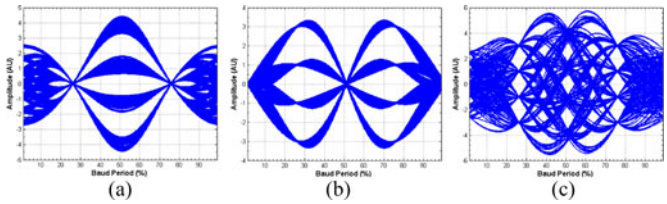

Fig. 6. Eye diag. of 25 Gb/s (a) PAM-4 (b) CAP-4Q (c) 50 Gb/s composite signal.

In orthogonal DWDM systems on the other hand, adjacent channels are continuously encoded with alternating in-phase and quadrature-phase CAP-Q channels, e.g., NRZ modulation on every 2*n*th channel and CAP-2Q on ever 2*n*–1th channel. Therefore, should two adjacent DWDM channels drift such that they are incident on an IM/DD receiver, they form orthogonal pairs and therefore don't suffer from the crosstalk levels experienced in MIMO DWDM systems. This means that DSP-hungry crosstalk cancellation and receiver diversity are no longer required. Should the worst case scenario then occur where channels drift to the point where a single AWG channel receives equal power contributions from 2 signals (+50 GHz drift of the wavelength grid in Fig. 2), the output of one of the AWG filters will be the composite eye of Figs. 5(c) or 6(c), depending on which coding scheme is employed. To then decode channels

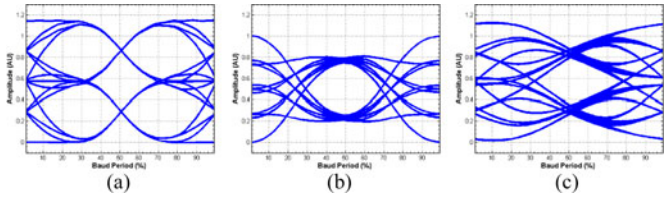

Fig. 7. Eye diag. of (a) agg. CAP-4 (b) decoded CAP-2Q (c) decoded NRZ.

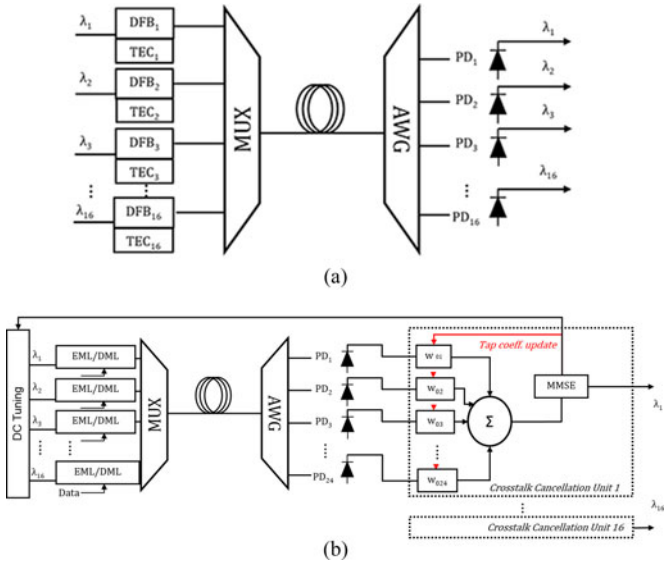

Fig. 8. 16 channel (a) Traditional. (b) MIMO DWDM.

for this scenario, a simple differential amplifier (2-tap transversal filter) or a 5-tap matched filter may be employed. For the in-phase channel, a low-pass filter can be used to improve eye opening. Shown above in Fig. 7(b), (c) are the decoded in-phase and quadrature channels as described in the worst-case scenario above and where the output of the AWG filter is the composite eye of Fig. 5(c), replicated in Fig. 7(a) again for completeness.

C. System Power Consumption

To gauge the potential impact that this technology might have on industry, we next compare the power consumption of a traditional DWDM system with that of the proposed orthogonal DWDM and the MIMO DWDM system previously reported. This analysis is done both on a per channel basis and in the context of next generation 400 Gigabit Ethernet which is likely to be ratified by the IEEE as its next standard [16], [17]. This working group is an extension of the previously ratified 100 GbE standard [2] and leverages on the success of 25 Gb/s modules. It is likely to be deployed using 16 DWDM channels to avoid exotic implementations. Shown in Fig. 8(a), (b) are exemplar systems for a typical DWDM system and an uncooled MIMO DWDM system, while the reader is advised to refer to Fig. 1 for the orthogonal DWDM system. Shown in Tables I–III are the power consumptions of the constituent subsystems allowing for a fair comparison of the traditional DWDM to MIMO DWDM and orthogonal DWDM systems.

TABLE I
POWER CONSUMPTION OF TRADITIONAL DWDM

Component	Power Consump. (mW/chan)	Total (W)	Ref
Transmitter			
LD[a]	*132*	*2.11*	
TEC[a]	*1125*	*18.00*	
Receiver			
PIN-TIA	*200*	*3.20*	[27]
CDR	*72*	*1.15*	[28]
TOTAL	1529	**24.46**	

[a] Measured values.

TABLE II
POWER CONSUMPTION OF MIMO DWDM

Component	Power Consump. (mW/chan)	Total (W)	Ref
Transmitter			
LD	*132*	*2.11*	
Receiver			
PIN-TIA	*1.5 × 200*	*4.80*	[27]
CDR	*1.5 × 72*	*1.73*	[28]
Crosstalk Canc.	*240*	*3.84*	[15]
TOTAL	780	**12.48**	
Power Saving		49%	

[b] assuming 1.5 times as many RX.
[c] assuming 24 tap crosstalk cancellation per channel.

TABLE III
POWER CONSUMPTION OF ORTHOGONAL DWDM

Component	Power Consump. (mW/chan)	Total (W)	Ref
Transmitter			
LD	*132*	*2.11*	
CAP modulator[d]	*5×10 = 50*	*0.80*	[15]
Receiver			
PIN-TIA	*200*	*3.20*	[27]
CAP decoder[e]	*2×10 = 20*	*0.32*	[15]
Channel control[f]	*2×10 = 20*	*0.32*	
CDR	*72*	*1.15*	[28]
TOTAL	494	**7.90**	
Power Saving[g]		68%	

[d] assuming CAP signal generation using 5 tap FFE.
[e] assuming CAP signal decoder requires differential amp. (2 tap).
[f] Controller used to choose correctly decoded signal.
[g] MZM consuming 600 mW [26] still offers ∼28% saving.

The results of the analysis are shown above in the second column. The clear reduction in power consumption of the orthogonal DWDM and MIMO DWDM schemes arise from the removal of TECs at the transmitter, which for a 16 channel DWDM system accounts for as much as 18 W. A DML laser source is assumed and all components fit within an SFP+ module such that a maximum power dissipation of < 2W is assumed. Orthogonal DWDM requires a slightly more complex transmitter than MIMO DWDM because of the requirements of having CAP-Q modulators fitted to lasers to enable CAP-Q modulation. These however come at a total increase of just 0.5 W, as a 5 tap transversal filter can be used to generate a CAP-Q signal, while a 2 tap differential amplifier can be used to decode it. Even though only every second channel requires

a CAP-Q modulator, additional redundancy is included so that should the case occur where channels drift at different rates so that a channel overtakes another, its modulation format can be readily controlled to maintain orthogonality. In a typical MIMO DWDM system, 1.5 times as many receivers to transmitters are used to avoid singularity issues. This means that for a 16-channel system, 24 receiving PIN diodes are required. Furthermore, the crosstalk cancellation unit has to be able to cancel crosstalk when the relative power ratios of two channels are nearly equal, this requiring the full channel matrix. While a MIMO DWDM system can theoretically achieve a power consumption saving of 49% compared with a traditional system, the DSP-based crosstalk cancellation units' requirements of having full channel state information leads to problems since its power consumption is expected to scale quadratically with channel number resulting in undesirable complexity. Orthogonal DWDM on the other hand does not require DSP and instead CAP-Q signals can be generated and decoded using low-cost transversal filters. A continuing issue for this system however, is the fact that CAP-Q channels have higher bandwidth requirements compared with in-phase channels along with the issues related to transient and adiabatic chirp in DMLs. The latter issue will result in additional penalty compared with using EML, however given that at 10 Gb/s, a 1 dB penalty due to adiabatic (transient) chirp is only found after 40 km (16 km) [18], this doesn't become a limiting factor considering data centre links are generally $<$10 km. In terms of bandwidth limitations, 40 Gb/s transmission of DML lasers is possible at temperatures as high as 85 °C [19] and 16 Gbaud PAM-4 shows only a $\sim$2 dB penalty compared with 13 Gbaud PAM-4 utilizing 10 Gb/s DML at a BER of 10^{-7} [20]. Even so, CAP modulation at 10 Gbaud 64-CAP over 20 km has recently been demonstrated using DML [21]. Finally, VCSELS with even lower power consumption have been shown to operate as high as 25 GHz [22] making them a cost-effective alternative. Nevertheless, even if MZM were to be used, a power consumption saving of $\sim$28% can still be achieved, while a $\sim$68% improvement in energy consumption over a traditional DWDM system is found using DMLs.

III. Experimental Results

A. 100 Gb/s (10 × 10 Gb/s) System Demonstration

Next, we review results of a proof-of-principle experiment [10] of a 10 × 10 Gb/s (aggregate 100 Gb/s) system that uses alternating NRZ and Manchester (CAP-2Q) channels for which the experimental setup is shown in Fig. 9.

Two sets of 5 optical carriers are coupled together, with channels in each set spaced by 200 GHz. These two sets are then modulated by two decorrelated 2^7-1 10 Gb/s NRZ and 10 Gb/s CAP-2Q PRBS sequences such that once the two sets are interleaved, adjacent channels are spaced by 100 GHz. Due to device limitations, instead of using a 5-tap transversal filter, CAP-2Q signals are generated using an XOR gate with the two differential inputs being the 10 Gb/s 2^7-1 PRBS sequence and a 10 GHz clock. This is known classically as Manchester coding but is analogous to CAP-2Q. CAP-2Q and an NRZ electrical

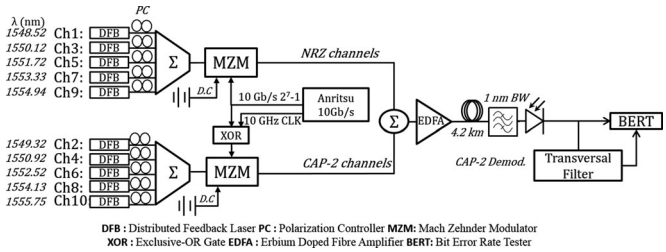

Fig. 9. 100 Gb/s Experimental setup.

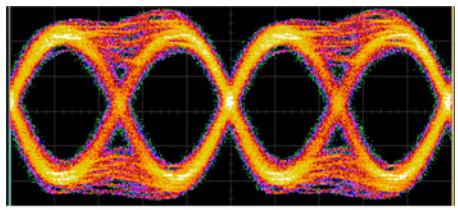

(a)

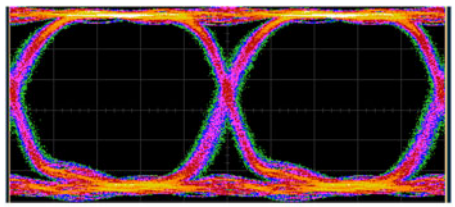

(b)

Fig. 10. Eye diagram (20 ps/div) for 10 Gb/s (a) CAP-2Q and (b) NRZ electrical signals.

eye diagram are shown in Fig. 10 below. The DWDM signal is then amplified using an EDFA to mitigate coupling losses.

At the receiver, a 1 nm filter is used to mimic the use of a broad bandwidth AWG channel and eye diagrams for all ten channels are shown in Fig. 11

Shown on the right hand side of Fig. 11 are NRZ channels and on the left hand side the CAP-2Q channels. The crosstalk from adjacent channels is apparent although error-free operation is easily possible in this best case scenario. The differences between channel crosstalk levels are due to unequalized variations in power levels of different channels.

In order to decode the CAP-2Q channels, the use of a prototype 5-tap transversal filter provided by Avago Technologies was employed. Only two of the five taps were used in the decoding process with tap coefficients set to $+1$ and -1. Shown in Fig. 12 is the decoded CAP-2Q channel from Channel 3.

Next, the back-to-back performance of CAP-2Q and NRZ are compared using single channel experiments. Low-cost photoreceiver that exhibit a BER of 10^{-12} at a received power of -12 dBm and an optical attenuator are employed to generate BER vs. received power graphs with and without the addition of 4.2 km of SMF. These are shown in Fig. 13.

In comparing the back-to-back BER curves for NRZ and CAP-2Q, it is clear that CAP-2Q suffers a high receiver sensitivity penalty. This arises from the poor performance of the transversal filter used. These are prototype devices, where

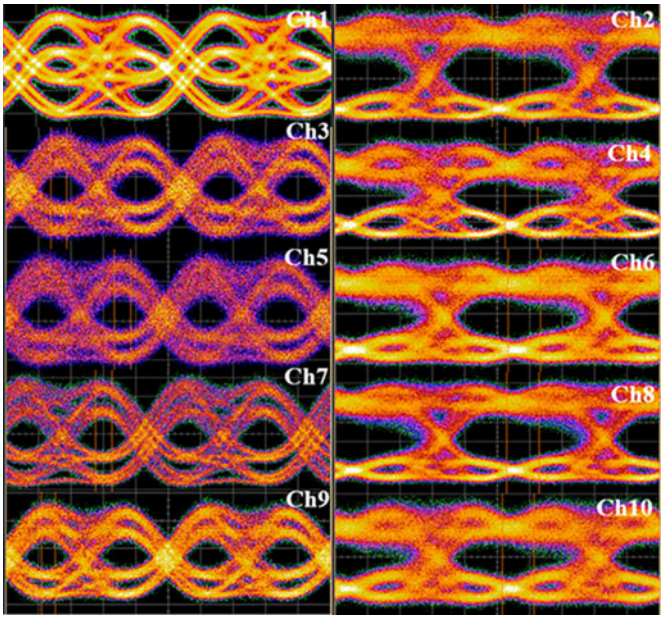

Fig. 11. Optical eye diagrams for (RHS) NRZ channels and (LHS) CAP-2Q channels (20 ps/div).

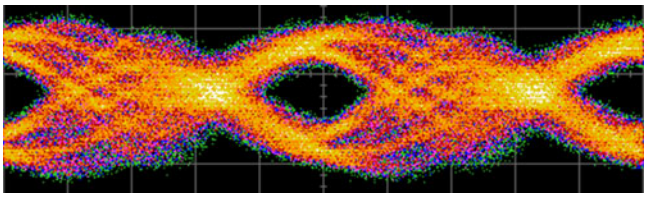

Fig. 12. Decoded CAP-2Q channel (20 ps/div).

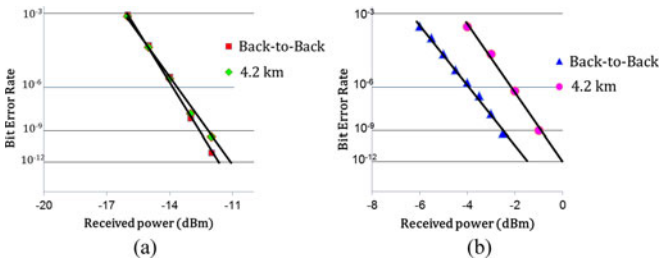

Fig. 13. (a) NRZ and (b) CAP-2Q BER versus received power plots with and without 4.2 km fiber.

the amplifiers that constitute the taps have unoptimized noise performance. By instead using limiting differential amplifiers [23] or a 20 Gb/s electrical 2:1 demultiplexer [24], a significant improvement is expected, with Manchester encoding showing a ~3 dB penalty compared with NRZ at 10 Gb/s at BER = 10^{-9}. Furthermore, a low-cost photodiode was used for this experiment, while a better one is likely to improve the sensitivity. Nevertheless, even with the addition of SMF, NRZ (CAP-2Q) only suffered an additional 0.2 (1.7) dB penalty making it suitable for short-reach applications.

The results of the experiment are shown in Fig. 14. Channels are set to drift in 4 steps of 25 GHz to simulate a system where channels drift from one AWG passband to another. At

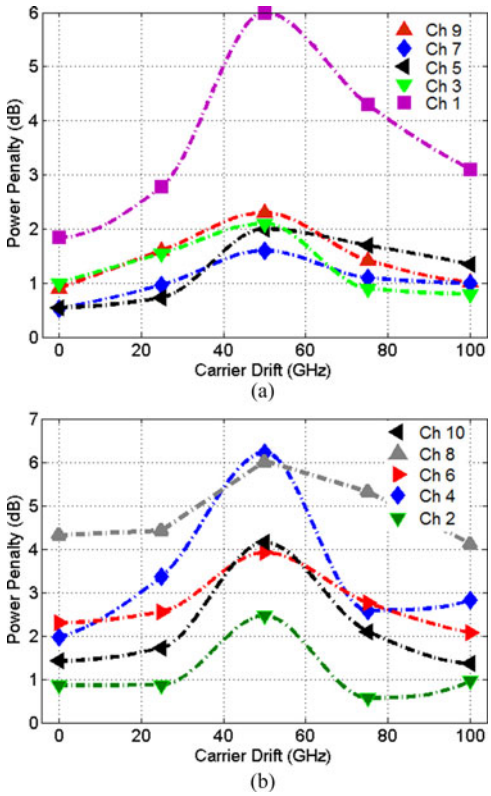

Fig. 14. Power penalties at a BER of 10^{-9} for (a) CAP-2Q and (b) NRZ channels.

each instant, BER vs. Received power curves are recorded and penalties at a BER of 10^{-9} plotted.

From the power penalty curves, it is evident that even in extremely challenging situations, i.e. once the wavelength grid drifts by 50 GHz to the AWG crossing points, error-free operation is still possible. In this situation, two adjacent channels fall within the passband of a single AWG detection channel with equal power and hence signals experience the maximum levels of crosstalk. NRZ (CAP-2Q) channels only experience a mean power penalty compared to back-to-back of 2.5 (4.5) dBm. This difference occurs because of the greater optical bandwidth that CAP-2Q signals resulting in greater crosstalk experienced by NRZ (Fig. 14).

B. Orthogonal DWDM Using Discrete Laser Sources

In practice, most DWDM systems employ discrete laser sources as opposed to integrated sources, these having different operating temperatures such that channels will drift at unequal rates depending on environmental factors. This can lead to scenarios where channels drift too close such that crosstalk and beat noise become detrimental. Occurrences of such situations can be detected and mitigated using channel identification and training protocols and corrected by current tuning lasers such that they maintain a predefined minimum channel separation. Laser tuning is possible at a rate of 1 GHz/mA. Furthermore, the requirement of having channels be temporally aligned within ±30% of the baud period can be accomplished using a combination of a training protocol and tunable phase shifters.

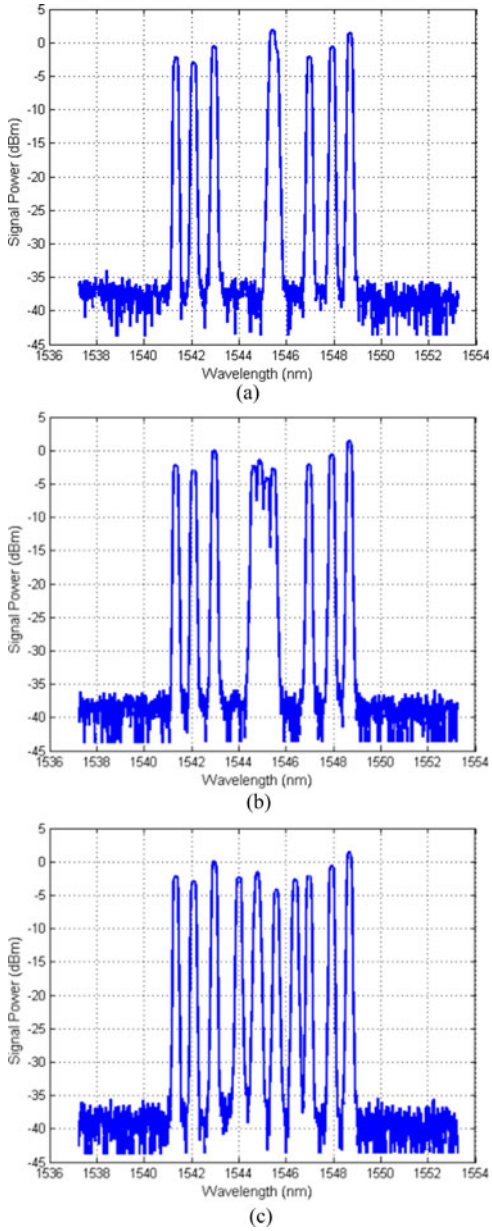

Fig. 15. (a) Initial conditions with 4 channels overlapping, (b) overlapping channels are biased to drift apart, and (c) channels are biased such that they have a 100 GHz channel spacing.

The feasibility of using discrete sources was tested experimentally in an aggregate 100 Gb/s (10 × 10 Gb/s) system, where the laser bias may be varied to optimize laser output wavelength. In this experiment, 10 channels are initially set to form a worst-case channel spacing where 4 of the 10 channels operate at the same wavelength such that their spectra overlap as shown in Fig. 15(a) below. These lasers are modulated using alternating CAP-2Q and NRZ modulation as before.

From here, lasers are iteratively biased such that they begin to drift apart (see Fig. 15(b)). Finally, lasers are biased appropriately such that they maintain a 100 GHz spacing as shown in Fig. 15(c).

From initial conditions where all channels overlap, 79 iterative steps are used to bias lasers such that they drift apart. After each of these steps, averaged waveforms are recorded from the 4 AWG filters and processed offline. Whereas in previous experiments, the BER was directly measured, here, an eye closure penalty is calculated by measuring the Q-factor of the signal and converting it to a BER as described by Eq. (1) below.

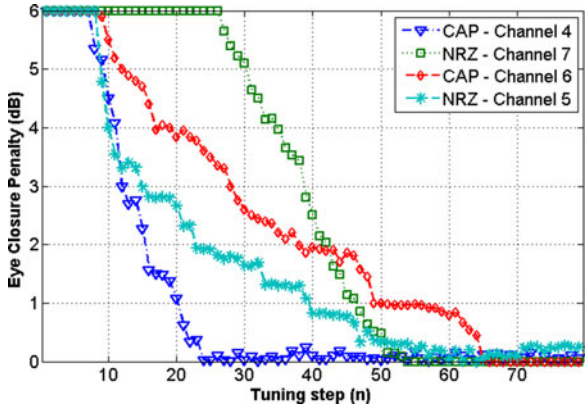

Fig. 16. Eye closure penalty for overlapping channels as they are biased.

Measurements assume a 10.3125 Gb/s 0.9 A/W p-i-n thermal noise dominated 10GBASE-LRM reference receiver with a 47.1 ps 20–80% rise time and −3 dB receiver bandwidth of 7.5 GHz. A receiver sensitivity of −18 dBm at a (BER) of 10^{-12} [12], [11], [13] is assumed. Assuming a 0 dBm launch power, a total power budget of 18 dB may be achieved. The transmitters are assumed to be single mode and so relative intensity noise (RIN) can be neglected. By varying the signal's power post-receiver, Q-factors are calculated from which BERs are derived as:

$$BER = \frac{1}{2} erfc\left(\frac{I_1 - I_0}{\sqrt{2\sigma_{th}}}\right). \quad (1)$$

Where σ_{th} is the thermal noise power at the received power and I_1 and I_0 represent 1 and 0 levels. The power required to achieve a BER of 10^{-12} is used to determine an eye closure penalty. Eye closure penalties for the 4 initially overlapping channels are shown in Fig. 16 below indicating that all channels can be appropriately biased such that they maintain a 100 GHz channel spacing allowing the penalty to be reduced to negligible levels. For each laser, the same amount of tuning current was used, however, due to device tuning differences this resulted in channels drifting at different rates, which explains the structure evident in the graph.

C. Pilot Tone Based Monitoring

Next, we discuss the need for channel identification and monitoring based on the simple method of pilot tone insertion [25]. Because channels are free to drift, invariably the case will arise where a channel drifts from one AWG filter's passband to the crossing point with an adjacent filter and then fully into its adjacent passband, this representing an 8 °C temperature rise. The system is designed to deal with this situation by including both an NRZ demodulator and a CAP demodulator. However, in order for the receiver subsystem to be aware of which of these receivers to use, pilot tones are inserted at as low as 10–200 kHz,

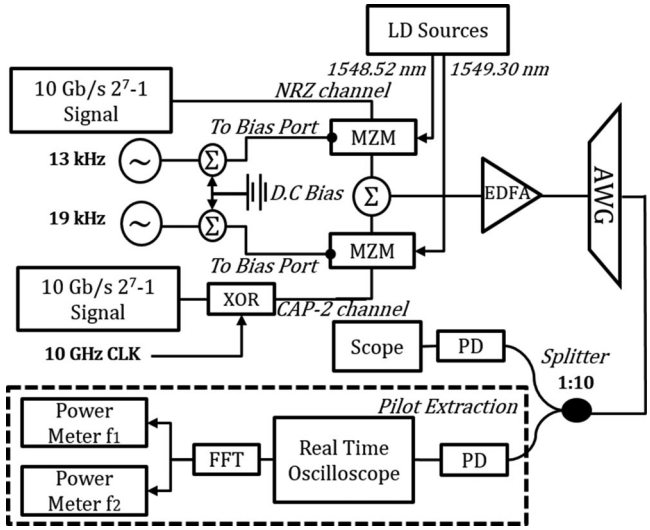

Fig. 17. Pilot tone experimental setup.

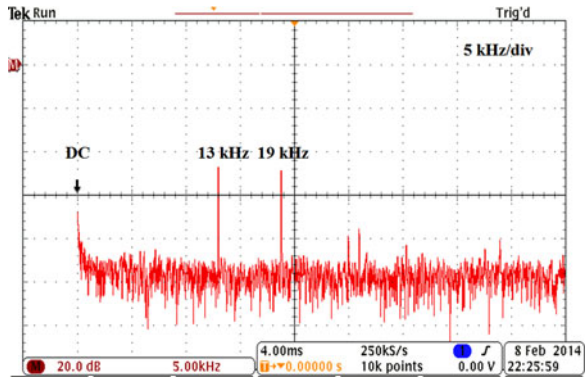

Fig. 18. Fourier transform plot showing pilot tones at 13 and 19 kHz (5 kHz/div).

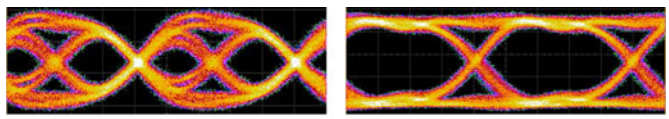

Fig. 19. Optical eye diagrams (20ps/div) of 10 Gb/s (a) CAP-2Q (b) NRZ channels with pilot tones.

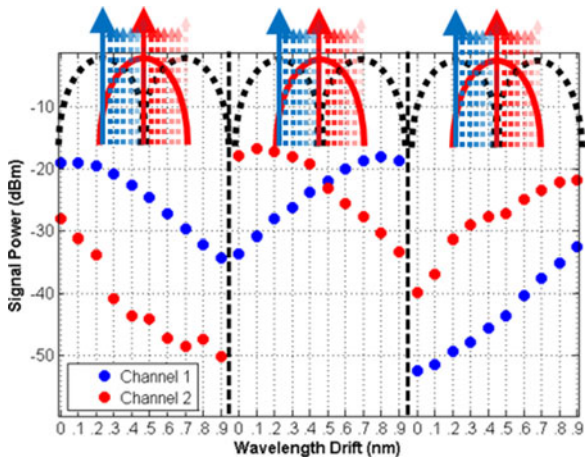

Fig. 20. Pilot tone powers versus wavelength drift for different AWG filters.

to minimize gain saturation effects of the EDFA. Pilot tones for optical channels are spaced by 6 kHz allowing channel identification and monitoring to occur. Should a channel then drift to an adjacent filter, the power of the pilot tone can be extracted and its information used to determine at what frequency the channel is currently operating and hence which receiver to use.

As shown in the experimental setup of Fig. 17, a 2 channel experiment is described where pilot tones at 13 and 19 kHz are introduced by a.c. coupling tones with a modulation index of 10% directly to the bias port of the MZM. 2 channels employing NRZ and CAP-2Q modulation at a channel spacing of 100 GHz are set to drift in ten iterations of 0.1 nm from one passband to another. A 1 nm optical filter with a second order Gaussian response is used to mimic the use of the broad passband AWG and channel wavelengths are swept three times with the center frequency of the filter changing 100 GHz for each separate sweep. Subsequently, a 1:10 splitter is used and one path is detected by a photodiode to allow eye diagrams to be analyzed on an oscilloscope while the other is fed to a photodiode connected to a 98 MHz low pass filter and detected by a 2.5 GSa/s real time oscilloscope.

The spectrum showing the two pilot tones without the addition of the 1 nm filter is shown in Fig. 18. Back-to-back optical eye diagrams of each channel with the inclusion of pilot tones are shown in Fig. 19 indicating minimal eye distortion.

For each iteration, waveforms are recorded for offline processing. The captured waveforms are processed using MATLAB where a 13 and 19 kHz bandpass filter with a -3 dB bandwidth of 2 kHz are synthesized to extract the pilots. The power of the pilot tones are calculated as channels drift, as shown by decreasing transparency in Fig. 20. For each of the 3 AWG filters, the signal power is plotted against wavelength drift in Fig. 20, where the inset figure shows which AWG filter is activated.

From the results of Fig. 20, it is clear that channel tracking is possible and the results may be used in combination with tapped electronics to allow receivers to overcome the ambiguity of which decoder output to use. Beginning with the 1st AWG filter in Fig. 20, as channels drift with increasing temperature from the initial starting wavelength to the passband of the adjacent filter, the power of the pilot tone of Channel 1 and Channel 2 reduce from -20 dBm (-29 dBm) to -34 dBm (-50 dBm), respectively. This shows that even when a channel is 200 GHz away, its power can be detected. This improves system fidelity as the power of a signal may be tracked from multiple sources allowing a better estimate of the channel wavelength to be estimated. For the second AWG filter, we see how channel 1 sees an increase in power from -34 dBm to a maximum of around -19 dBm before tailing off, while an almost mirror image is seen for Channel 2. The tailing off can be explained because after a drift of 0.8 nm, Channel 2 has drifted beyond the center wavelength of the filter where its power begins to fall. The point at which the signal powers of Channel 1 and 2 cross is the point where channels have drifted to the crossing points of adjacent

AWGs and the signals exhibit equal power contribution on the AWG of interest. This is in good agreement with expectations as this point occurs at a wavelength grid drift of 50 GHz.

For the final AWG filter, channel 2 drifts from the passband of the middle AWG to the third AWG, a scenario similar to the case just mentioned where Channel 1 drifts from the first AWG to the second. Here again we see a similar trend in a rising pilot tone power as drift occurs. For Channel 2, which is 200 GHz away from the center frequency of this AWG filter, a pilot tone power of -52 dBm is calculated and we see a rising trend to just below -30 dBm in good agreement with its starting power in the middle AWG. Slight deviations from expectations can be explained by the accuracy with which the center frequencies of the 1 nm filter used to mimic the AWG (± 0.05 nm) as well as inaccuracies in setting the wavelength of the lasers (± 0.05 nm). We can thus easily distinguish between tones and should the experiment be altered to include even more channels, similar results are to be expected. This data can then be used by the receiver which can then choose if the NRZ decoder or the CAP-2Q decoder is to be used to demodulate signals.

IV. Conclusion

We have described the use of orthogonal coding schemes on adjacent carriers in a DWDM network using discrete sources and have found that by using a broad bandwidth AWG filter with overlapping spectra and slow roll-offs, channels can still be detected even in the most challenging of cases, i.e. when channels drift to filter crossing points. This means that TECs at the transmitter are no longer required allowing for a power consumption saving of 68% to be realized. Experimentally, it is found that CAP-2Q signals are more resilient to crosstalk from NRZ channels and a 100 Gb/s aggregate (10×10 Gb/s) system experiences a mean maximum penalty of just 2.5 dB compared to NRZ which exhibited a mean penalty of 4.5 dB. Discrete lasers with different rates can be employed and biasing of lasers in combination with channel identification and tracking employing pilot tones at anywhere from 10 to 200 kHz used to avoid situations where channels drift too close. Channel identification also allows the receiver to know whether to process a channel as an NRZ or CAP-2Q signal.

Acknowledgment

The authors would like to thank the Engineering and Physical Science Research Council (EPSRC) and Corning for awarding the author the grand prize best student paper at OFC 2014.

References

[1] D. J Law, W. W. Diab, A. Healey, S. B. Carlson, and V. Maguire, "IEEE 802.3 industry connections Ethernet bandwidth assessment," IEEE 802.3 Ethernet Work. Group, San Diego, CA, USA, 2012.

[2] IEEE 802.3ba, "40 Gb/s and 100 Gb/s Ethernet," 2010.

[3] G. Boccaletti, M. Löffler, and J. M. Oppenheim, "How IT can cut carbon emissions," *McKinsey Quart.*, 2008. [Online]. Available: https://www.mckinseyquarterly.com/How_IT_can_cut_carbon_emissions_2221

[4] T. Kelly, "ICTs and climate change," *ITU-T Technology, Tech. Rep.*, (2007, Dec.) [Online]. Available: http://www.itu.int/themes/climate/docs/report/02_ICTandClimateChange.html

[5] C. A. Brackett, "Dense wavelength division multiplexing networks: Principles and applications," *IEEE J. Sel. Areas Commun.*, vol. 8, no. 6, pp. 948–964, Aug. 1990.

[6] S. L Chuang, "Distributed feedback lasers," in *Physics of Photonic Devices*, Hoboken, NJ, USA: Wiley, 2009, p. 502.

[7] S. H. Lee, A. Wonfor, R. V. Penty, I. H. White, G. Busico, R. Cush, and M. Wale, "Uncooled DWDM transmission system using tunable laser sources with anti-mode-hop control protocol," presented at the IEEE Photon. Conf., New York, NY, USA, 2011.

[8] S. H. Lee, D. G. Cunningham, R. V. Penty, and I. H. White, "Uncooled MIMO WDM system using advanced receiver signal processing techniques," presented at the SPIE Photon. West, San Francisco, CA, USA, 2012.

[9] J. D. Ingham, S. H. Lee, R. V. Penty, I. H. White, and D. G. Cunningham, "100 Gb/s uncooled WDM system using conventional WDM components and advanced receiver signal processing," presented at the Eur. Conf. Opt. Commun., Amsterdam, The Netherlands, 2012.

[10] J. B. von Lindeiner, J. D. Ingham, A. Wonfor, J. Zhu, R. V. Penty, and I. H. White, "100 Gb/s uncooled DWDM using orthogonal coding for low-cost datacommunication links," presented at the Opt. Fiber Commun., San Fransisco, CA, USA, 2014.

[11] J. L. Wei, D. G. Cunningham, R. V. Penty, and I. H. White, "Study of 100 Gigabit Ethernet using carrierless amplitude/phase modulation and optical OFDM," *J. Lightw. Technol.*, vol. 31, no. 9, pp. 1367–1373, May 2013.

[12] J. D. Ingham, R. V. Penty, and I. H. White, "40 Gb/s carrierless amplitude and phase modulation for low-cost optical data communication links," presented at the Opt. Fiber Commun./Nat. Fiber Opt. Eng. Conf, Los Angeles, CA, USA, 2011.

[13] I. H. White, J. D. Ingham, and R. V. Penty, "Systems aspects of optical technologies for use in data communications," presented at the Opt. Fiber Commun./Nat. Fiber Opt. Eng. Conf., Los Angeles, CA, USA, 2011.

[14] J. J. Werner, "Tutorial on carrierless AM/PM - Part III," ANSI X3T9.5 TPlPMD Work. Group, 1993.

[15] C. L. Schow *et al.*, "Transmitter pre-distortion for simultaneous improvements in bit-rate, sensitivity, jitter, and power efficiency in 20 Gb/s CMOS-driven VCSEL links," presented at the Opt. Fiber Commun./Nat. Fiber Opt. Eng. Conf., Los Angeles, CA, USA, 2011.

[16] J. D'Ambrosia, "Ethernet's next step: 400 Gigabit Ethernet," presented at the Ethernet Technol. Summit, Santa Clara, CA, USA, 2013.

[17] J. D'Ambrosia, "100 Gigabit Ethernet and beyond," *IEEE Commun. Mag*, vol. 48, no. 3, pp. S6–S13, Mar. 2010.

[18] I. Papagiannakis *et al.*, "Performance of 2.5 Gb/s and 10 Gb/s transient and adiabatic chirped directly modulated lasers using electronic dispersion compensation," presented at the Eur. Conf. Opt. Commun., Berlin, Germany, 2007.

[19] A. Uetake *et al.*, "40 Gpbs direct modulation of 1.55 um AlGaInAs semi-insulating buried heterostructure distributed reflector lasers up to 85 °C," in presented at the Annu. Meeting Lasers Electro-Opt. Soc., Belek-Antalya, Turkey, 2009.

[20] X. Song and D. Dove, "Opportunities for PAM4 moduation," IEEE 802.3 400 GbE Study Group, 2014.

[21] J. Zhang *et al.*, "60-Gb/s CAP-64QAM transmission using DML with direct detection and digital equalization," presented at the Opt. Fiber Commun., San Francisco, CA, USA, 2014.

[22] R. Rodes *et al.*, "High-speed 1550 nm VCSEL data transmission link employing 25 GBd 4-PAM modulation and hard decision forward error correction," *J. Lightw. Technol.*, vol. 31, no. 4, pp. 689–695, Feb. 2013.

[23] S. H Lee *et al.*, "Coarse optical orthogonal frequency division multiplexing for optical datacommunication applications," presented at the Conf. Lasers Electro-Opt., Baltimore, MD, USA, 2011.

[24] J. Zhang, N. Chi, P. V. Holm-Nielsen, C. Peucheret, and P. Jeppesen, "Method for high-speed Manchester encoded optical signal generation," presented at the c. Opt. Fiber Commun. Conf., Los Angeles, CA, USA, 2004.

[25] K. J. Park, S. K. Shin, and Y. C. Chung, "Simple monitoring technique for WDM networks," *Electron. Lett.*, vol. 35, no. 5, pp. 415–417, Mar. 1999.

[26] S. Bhoja, (2012, 23–27 Jan.). Study of PAM modulation for 100GE over a single laser. [Online]. Available: http://www.ieee802.org/3/100GNGOPTX/public/jan12/bhoja_01_0112_NG100GOPTX.pdf.

[27] J. D. Ingham, R. V. Penty, I. H. White, and D. G. Cunningham. (2012, Jul.). Multipulse modulation schemes for 100 Gigabit Ethernet.[Online]. Available: http://www.ieee802.org/3/100GNGOPTX/public/jul12/ingham_01a_0712_optx.pdf

[28] J. Savoj and B. Razavi, "A 10-Gb/s CMOS clock and data recovery circuit with a half-rate linear phase detector," *IEEE J. Solid-State Circuit*, vol. 36, no. 5, pp. 761–768, May 2001.

Johannes Benedikt von Lindeiner received the M.Eng. degree in electronic and electrical engineering and the M.Res. degree in photonic systems development from UCL, London, U.K., in 2010 and 2011, respectively. He is currently working toward the Ph.D. degree with the Centre for Photonic Systems, Electrical Engineering Division, University of Cambridge, Cambridge, U.K., and is currently a Researcher intern at Alcatel-Lucent Bell Labs, Murray Hill, NJ, USA. He received the 2014 Grand Prize of the Corning Outstanding Student paper at OFC 14', as well the 2014 Cullen Prize, is the Founder and President of the Cambridge University OSA Student Chapter and is a Reviewer for the IEEE JOURNAL OF LIGHTWAVE TECHNOLOGY.

Jonathan D. Ingham (M'99) received the M.A. degree from the University of Cambridge, Cambridge, U.K., and the Ph.D. degree from the University of Bristol, Bristol, U.K. He read electrical and electronic engineering at Imperial College London, and received the Ph.D. degree from the University of Bristol before joining the Department of Engineering, University of Cambridge, Cambridge, U.K. He has authored more than 70 peer-reviewed papers in leading journals and conferences.

Adrian Wonfor (M'02) received the B.Sc. degree in physics from the University of Bath, Somerset, England, U.K., in 1992. He is a Senior Research Associate at the Centre for Photonic Systems, Engineering Department, University of Cambridge, Cambridge, U.K. He is the author or coauthor of more than 100 publications and is the holder of several patents.

Jiannan Zhu received the B.Sc. degree in electrical and electronic engineering from the Huazhong University of Science and Technology, Wuhan, China, in 2011. He is currently working toward the Ph.D. degree at the Centre for Photonic Systems, Engineering Department, University of Cambridge, Cambridge, U.K. His current research interests include datacoms and passive optical networks.

Richard V. Penty (SM'10) received the Ph.D. degree from the University of Cambridge, Cambridge, U.K., in 1989. He is currently Master of Sidney Sussex College. He was a Science and Engineering Research Council Information Technology Fellow at the University of Cambridge, where he is currently a Professor of Photonics. He has held academic posts at the University of Bath, Bath, U.K., and the University of Bristol, Bristol, U.K. He is the author or coauthor of more than 700 publications. He is the Editor-in-Chief of the Institution of Engineering and Technology Optoelectronics Journal and Founder of Zinwave Ltd.

Ian H. White (S'82–M'83–SM'00–F'05) received the B.A. and Ph.D. degrees from the University of Cambridge, Cambridge, U.K., in 1980 and 1984, respectively. He is currently Master of Jesus College, van Eck Professor of Engineering, Deputy Vice-Chancellor, and the Head of Photonics Research at the Department of Engineering, University of Cambridge. He was a Member of the Board of Governors of the IEEE Photonics Society (2008–2012) and is the Editor-in-Chief of *Electronics Letters*. He has published in excess of 800 publications and holds 28 patents.